Bioorganic Chemistry 81 (2018) 71–78

Contents lists available at ScienceDirect

Bioorganic Chemistry

journal homepage: www.elsevier.com/locate/bioorg

DNA-binding, enzyme inhibition, and photochemical properties of chalcone-containing metallophthalocyanine compounds

Furkan Özen[c], Aslıhan Günel[b], Arif Baran[a,*]

[a] Sakarya University, Faculty of Arts and Sciences, Chemistry Department, 54187 Sakarya, Turkey
[b] Ahi Evran University, Faculty of Arts and Sciences, Chemistry Department, 40100 Kırşehir, Turkey
[c] Akdeniz University, Faculty of Education, Antalya 07058, Turkey

ARTICLE INFO

Keywords:
Phthalocyanine
Chalcone
Enzyme inhibition
DNA-binding
Photochemical

ABSTRACT

In this study, two novel phthalocyanine complexes were synthesized using their corresponding metal salts and 4-(4-(3-(2,4,5-trimethoxyphenyl)acryloyl)phenoxy)phthalo-nitrile as chalcone ligand (**4**), which was prepared from the reaction of 4-nitrophthalonitrile with 4-hydroxyphenyl-3-(2,4,5-trimethoxyphenyl)prop-2-en-1-one (**3**). These metallophthalocyanines showed good solubility in organic solvents such as $CDCl_3$, DCM, THF, DMF, and DMSO. The novel phthalocyanine compounds **4a** (Pc-Zn) and **4b** (Pc-Co) were characterized using their UV–vis, FT-IR, ^{1}H NMR, ^{13}C NMR, and MALDI-TOF mass spectra and elemental analysis. Then the DNA-binding and xanthine oxidase and carbonic anhydrase-I inhibition properties of compounds **4a** and **4b** were investigated. Photochemical properties (such as singlet oxygen generation and photodegradation) of this novel chalcone phthalocyanine (**4a**) were determined in dimethyl sulfoxide (DMSO).

1. Introduction

Phthalocyanines (Pcs) have been extensively studied due to their distinct applications, including pigments and dyes [1], chemical sensors [2], photodynamic therapy sensitizers [3], optical recording and non-linear optical materials [4], photovoltaics, [5] catalysts [6], electrochromic materials [7], electronic device components [8], electrochemical applications [9], enzyme inhibition [10,11], and photochemical [12] and photodynamic therapy [13].

Chalconoids, are natural compounds belonging to the flavonoids. Chalcones can be easily prepared by Claisen–Schmidt condensation as mentioned [14,15]. They exhibit electrochromic properties [16], fluorescence properties [17], thermal and dielectric properties [18,19], antimicrobial [20], anti-HIV [21,22], antibacterial [23], anti-inflammatory [24,25], and anticancer activity [26,27], and also DNA-binding [28] and enzyme inhibition [29,30]. As stated in the literature, chalcone compounds are biologically active molecules. In addition, since chalcones are compounds having good solubility, they are used as ligands in the synthesis of phthalocyanine compounds. There have been exciting developments in the treatment of cancer in recent years, but it still has not reached the desired level. The interaction of DNA with metal complexes has been an important research topic. DNA is extremely negatively charged. For this reason, a strong interaction with oppositely charged species occurs. Therefore, the interaction of cationically charged phthalocyanines with DNA has attracted considerable interest in recent years [31–35].

There are several studies on phthalocyanine compounds containing chalcone [36–43]. In the present study, DNA-binding and enzyme-inhibition studies were carried out differently from the literature and a new study on phthalocyanines containing chalcone was performed. The synthesis and characterization of new novel Pc-Zn (**4a**) and Pc-Co (**4b**) compounds interdependent with 4-(4-(3-(2,4,5-trimethoxyphenyl)-acryloyl)phenoxy)phthalonitrile (**4**) units were conducted. Aims of the study were therefore the synthesis and characterization of new metallophthalocyanine compounds containing chalcone and study of their some spectral and photochemical properties.

2. Result and discussion

2.1. Synthesis and characterization

4-Hydroxyphenyl-3-(2,4,5-trimethoxyphenyl)prop-2-en-1-one (**3**) was prepared according to a method reported [15,44]. 4-(4-(3-(2,4,5-trimethoxyphenyl)-acryloyl)phenoxy)-phthalonitrile (**4**) was prepared and used as a starting material for the preparation of novel mono phthalocyanines. The synthetic route of the new phthalocyanines can be exhibit in Scheme 1. The novel compounds of phthalocyanine showed good solubility in different solvents (acetone, DCM, THF, DMF,

* Corresponding author.
E-mail address: abaran@sakarya.edu.tr (A. Baran).

https://doi.org/10.1016/j.bioorg.2018.08.002
Received 9 June 2018; Received in revised form 1 August 2018; Accepted 3 August 2018
Available online 04 August 2018
0045-2068/

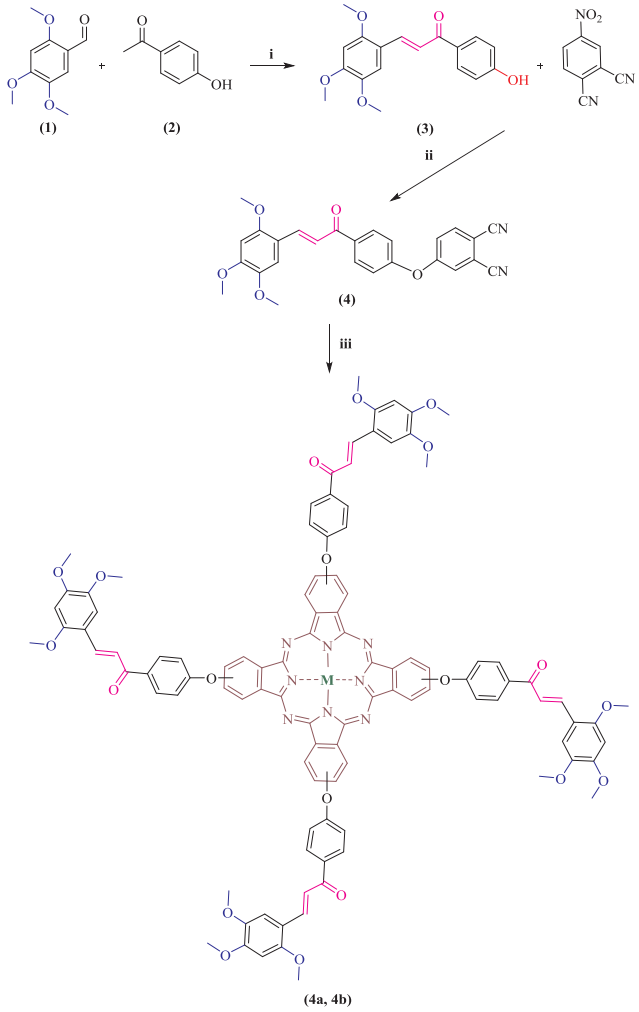

Scheme 1. Synthetic route of compounds **3, 4, 4a**, and **4b**. (i) KOH 10%, EtOH, r.t., 24 h; (ii) K_2CO_3, DMF, 50 °C; (iii) **4a** $Zn(OAc)_2{\cdot}2H_2O$, DMF, 140 °C, 12 h; **4b** $Co(OAc)_2{\cdot}4H_2O$, DMF, 140 °C, 12 h.

and DMSO). The compounds **4a** and **4b** were characterized using their UV–vis, FT-IR, ^{1}H NMR, ^{13}C NMR, and MALDI-TOF. The IR spectra of compound **4** show aromatic (Ar—H) peak at 3069 cm^{-1}; aliphatic (C—H) peak at 2939 cm^{-1}; (C≡N) peak at 2229 cm^{-1}; (C=O) peak at 1656 cm^{-1}; (C=C) peak at 1608, 1584 cm^{-1}. The absence of the O—H peak at 3284 cm^{-1} in the spectrum and the formation of the C≡N peak at 2229 cm^{-1} indicate the formation of **4** compounds. No observation of the peak at 2229 cm^{-1} (C≡N) in the spectrum of compounds **4a** and **4b** shows that the compounds are phthalocyanine.

The NMR data of compounds **3** and **4** are detailed in the experimental section. In the ^{1}H NMR spectrum the compounds data also confirm the structures of **3** and **4**. The aromatic protons for all the compounds exhibit between 8.15 and 6.52 ppm. The methoxy protons for compounds **3** and **4** were observed at 3.94, 3.90, and 3.89 ppm, respectively. The integral heights in the spectrum of compound **4** confirm the numbers of protons as well. The ^{13}C NMR spectral data are given in the experimental section. The carbonyl carbon atoms for **3** and **4** were appeared at 190.43 and 189.57 ppm, respectively. The aromatic carbon atoms appear between 160.96 and 96.87 ppm. The methoxy carbons for compounds **3** and **4** were observed at around 56.80 and 56.20 ppm, respectively. UV–vis spectra are the best indication for phthalocyanine compounds. Generally, two absorption bands are observed in the electronic absorption spectrum of phthalocyanine compounds. One of them is in the visible region at about 300–450 nm in the B band and the other one is in the visible region at 600–750 nm in the

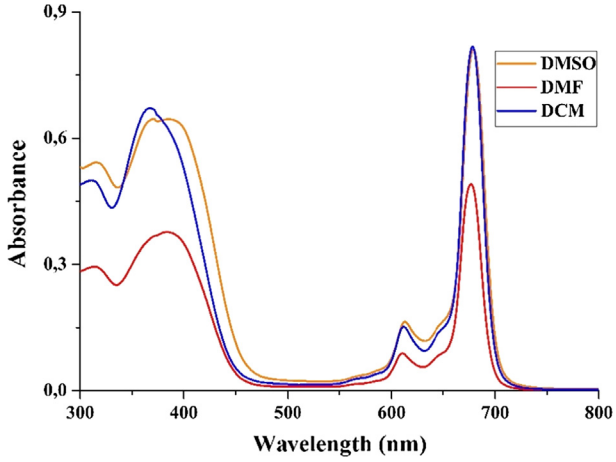

Fig. 1. UV–vis of compound **4a** (1×10^{-5} mol/dm^3) in different solutions.

Q-band. The Q-band is bonded to the $\pi \rightarrow \pi^*$ transition from the highest occupied molecular orbital (HOMO) to the lowest unoccupied molecular orbital (LUMO) of the phthalocyanine ring. The B-band absorptions are observed from deeper π levels to the LUMO transitions. In the present study, the phthalocyanine complexes **4a** and **4b** in different solvents (DMSO, DMF, DCM) showed characteristic absorption regions; one of them is in the UV region at about 360–385 nm in the B-band region and the other one is in the visible region at 580–700 nm in the Q-band region (Figs. 1 and 2). The mass spectra of phthalocyanines **4a** and **4b** were also recorded. Molecular ion peaks were identified at $m/z = 1828.10$ as the $[M+H]^+$ for **4a** and $m/z = 1821.05$ as the $[M+H]^+$ for **4b**. Molecular ion peaks in the mass spectra support the proposed molecular formula.

2.2. DNA binding studies

2.2.1. Fluorescence spectroscopic studies

Binding constant ***(K_f)*** and **n** values are calculated by drawing a chart of ***log (F_o − F)/F*** versus ***log [Q]***. ***K_f*** is obtained by dividing the intercept by the slope and the ***n*** value is the slope of the plot [45]. The plot of ***(F_o − F)/F*** versus ***log [Q]*** is given for **4a** and **4b**, respectively (Figs. 3 and 4). The results are shown in Table 1.

Fig. 3 shows the fluorescence spectrum emission spectra of **4a** in the presence of DNA in 5 mM Tris-HCl (pH 7.4) buffer. The arrow represent intensity changes on the increase in DNA concentration.

Fig. 4 shows the fluorescence spectrum emission spectra of **4b** in the presence of DNA in 5 mM Tris-HCl (pH 7.4) buffer. The arrow represent

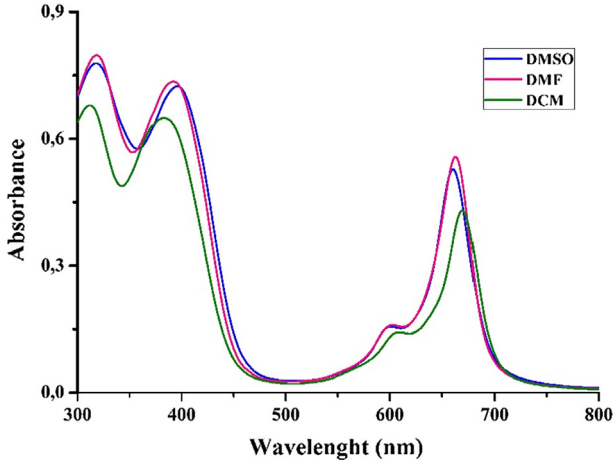

Fig. 2. UV–vis of compound **4b** (1×10^{-5} mol/dm^3) in different solutions.

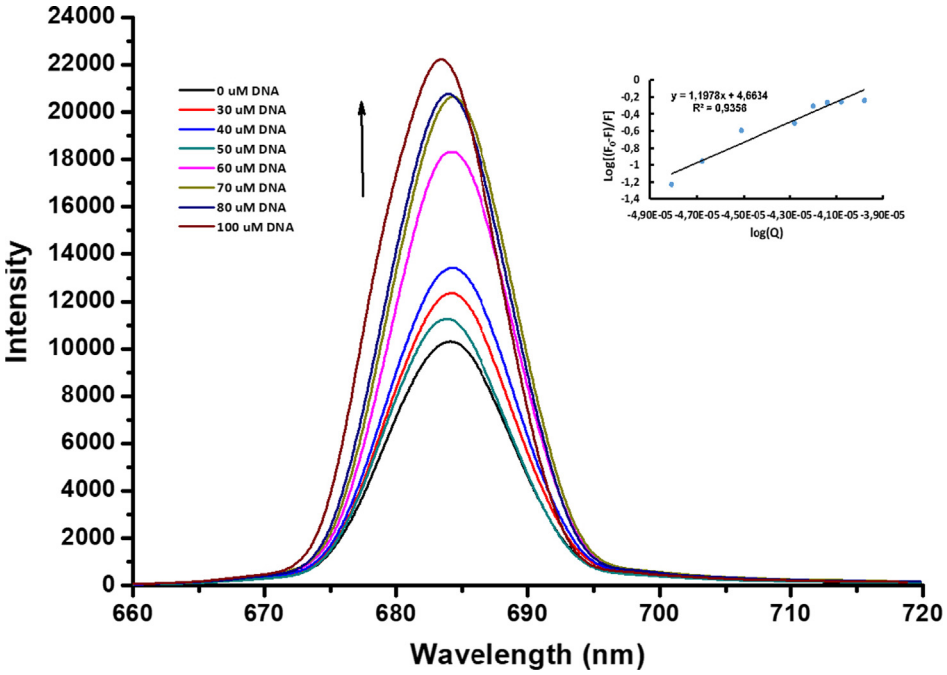

Fig. 3. Fluorescence spectrum emission spectra of the plot of $(F_0 - F)/F$ versus log [Q] of **4a**.

intensity changes on the increase in DNA concentration.

When we titrate the **4a** complex with increasing DNA concentration, fluorescence intensity is increased. This means **4a** complex binds to DNA in a hyperchromic manner. DNA structure and confirmation were changed by an agent that possesses the hyperchromic feature because DNA double strands open and these molecules with the intercalator property intervene between the DNA strands. Titration of **4b** with rising DNA concentration results in decreasing fluorescence intensity; this effect is named the hypochromic effect. The molecules binding to DNA with hypochromicity exhibit electrostatic, hydrogen bonding, and hydrophobic interactions and therefore these molecules approximate to the sugar-phosphate backbone. These kinds of agents are generally groove binders [46].

Table 1
Binding characteristic of **4a** and **4b** complexes with CT-DNA.

Compound	$K_f/(L\,mol^{-1})$	n
4a	7821.75	1.20
4b	8113.34	0.67

2.2.2. Enzyme inhibition assay

Xanthine oxidase inhibition activity of **4a** and **4b** was studied between 0.125 and 20 μM concentration. The results are presented in Table 2.

The best enzyme inhibition activity was observed with **4a** derivative and the IC_{50} value of this compound was 0.290 μM.

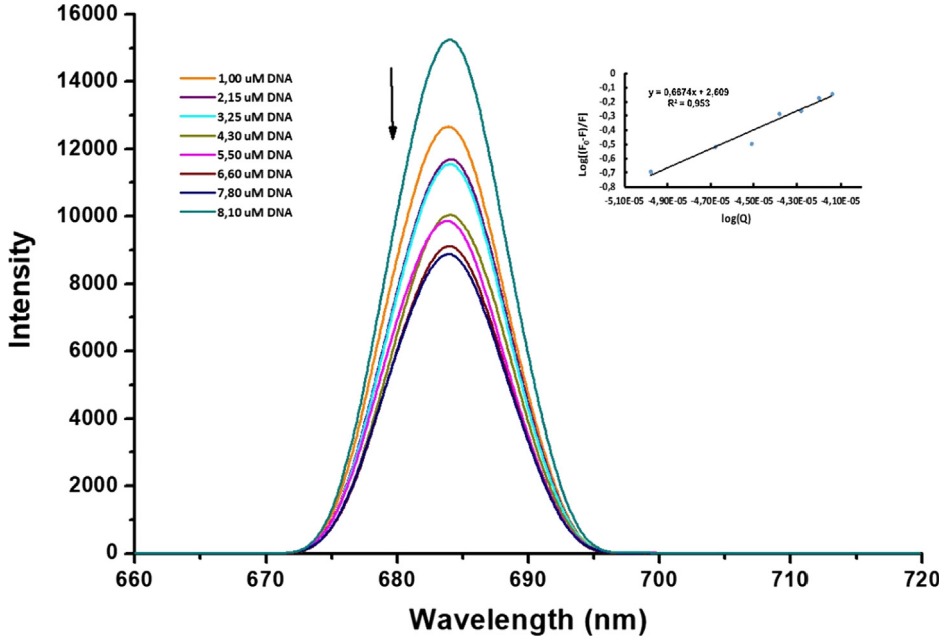

Fig. 4. Fluorescence spectrum emission spectra of the plot of $(F_0 - F)/F$ versus log [Q] of **4b**.

Table 2
Inhibition properties of phthalocyanine derivatives against xanthine oxidase.

Compound	Percentage xanthine oxidase inhibition								IC_{50}
Concentration (μM)	0.125	0.250	0.375	0.4	0.45	10	15	20	
4a	27.45	28.43	65.69	72.55	84.22	–	–	–	0.290
4b	–	–	–	–	–	12.02	17.05	17.09	ND*
Allopurinol									5.038#

Allopurinol was used as positive control for xanthine oxidase inhibition and concentration range was 1–25 μM.
* IC_{50} value could not be determined.

Table 3
Inhibition properties of phthalocyanine derivatives against carbonic anhydrase.

Compound	Percentage carbonic anhydrase-I inhibition				IC_{50}
Concentration (μM)	0.625	2.500	3.125	3.750	
4a	27.08	51.04	75.0	81.25	1.69
4b	–	–	–	–	ND*
Acetazolamide	–	–	–	–	7.07#

Acetazolamide was used as positive control for carbonic anhydrase inhibition and concentration range was 1–13.5 μM.
* IC_{50} value could not be determined.

A carbonic anhydrase inhibition assay was performed for the two compounds and inhibition activity was observed just for **4a** in very low concentrations, whereas no inhibition effect was observed for the other compound (**4b**) although concentration was increased up to 100 μM (Table 3) [47,48].

Both xanthine oxidase inhibitors and carbonic anhydrase inhibitors are important drug candidates for several diseases such as epilepsy [49], altitude diseases [50], and glaucoma [51]. Moreover, several isoforms of carbonic anhydrase have anticancer activity such as against breast cancer [52], prostate cancer [53], and kidney cancers [54]. The best enzyme inhibition activity was exhibited by **4a** for both enzymes. Compound **4b** exhibited inhibition activity against xanthine oxidase even in very small percentages, but carbonic anhydrase was inhibited by just **4a**. Acetazolamide is an approved and effective inhibitor for carbonic anhydrase-I and we calculated the IC_{50} value for this compound as 7.07 μM and compound **4a** exhibits better inhibition according to acetazolamide. Zn^{2+} ion in the complex might compete with Zn of the enzyme active site. In the complexes, Zn^{2+} forms complex by binding N atom of each ligand also carbonic anhydrase is a metalloenzyme and it contains Zn^{2+} ion and surrounded by three histidine residue and water molecule. When Complex 4a containing Zn^{2+} ion is added to reaction media metal ion of complex might replace by metal ion found in active site of enzyme. On the other hand, we cannot speculate similar situation for complex 4b. Our results thus indicate that compound **4a** is a strong CA inhibitor that may be used as a lead for generating more powerful CA inhibitors in further studies.

In our study, the xanthine oxidase IC_{50} value for allopurinol was 5.038 μM whereas compound **4a** had an IC_{50} value of 0.290 μM. Compound **4a** has crucial inhibition peculiar for this enzyme according to the positive control. Xanthine oxidase has three major domains; Fe/S domain, FAD-binding domain and molybdopterin center [55]. Complex 4a is a promising agent for xanthine oxidase inhibition whereas 4b shows inhibition effect less than almost 100 times of 4a. These two compounds have similar structure except coordination metals, molybdopterin region is crucial for xanthine oxidase activity. Compounds with metal ions can act as antagonistic for molybdenum in molybdepterin domain. It is declared that some compounds with Zn and Cu are decreased uric acid level importantly and also xanthine oxidase activity by preventing oxidation of xanthine, physiological substrate of the enzyme [56]. In the light of these literature we can suggest that metal ion is responsible for inactivity of the enzyme.

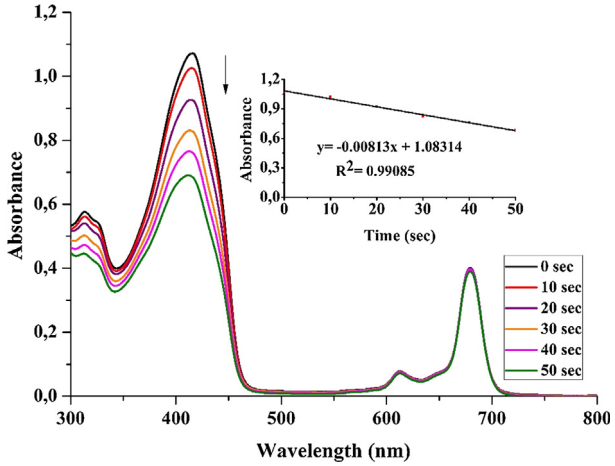

Fig. 5. Change observed in UV–vis spectrum during measurement of singlet oxygen quantum yield of compound **4a** in DMSO.

2.3. Photochemical studies

2.3.1. Singlet oxygen quantum yield (Φ_Δ)

A solution of compound **4a** in DMSO was prepared at a concentration of 1×10^{-5} M for singlet oxygen quantum yield. 1,3-Diphenylisobenzofuran (DPBF) was added as a singlet oxygen extinguisher in solution of **4a** in the dark. This mixture, which was prepared later, was left out of light at a certain time interval of 8.15×10^{15} photon s^{-1} cm^{-2}. Absorption change at 417 nm of DPBF from the UV–vis spectrum was observed (Fig. 5).

No change in the Q band was observed in the singlet oxygen quantum yield measurement. The calculated result for Φ_Δ is close to the value in the literature. The singlet oxygen quantum yield of compound **4a** was calculated as seen from Table 4. As a result, this study indicates the potential of compound **4a** as a photosensitizer in applications of PDTs.

2.3.2. Photodegradation and quantum yield (Φ_d)

While photodegradation shows resistance to the emission of molecular light, a series of chemical reactions such as dehydrogenation, dehydromethylation occur. Also, it may cause the formation of chromophore groups such as carbonyls, carboxyls, peroxides, and conjugated bonds. The singlet oxygen formed during photooxidation of phthalocyanine compounds is exposed to depolymerization by introducing into the ring of phthalocyanine and separation reactions

Table 4
Photochemical parameters of **4a** in DMSO.

Compound	Φ_Δ	Φ_d
4a	0.53	8.9×10^{-4}
ZnPc[a]	0.56	2.3×10^{-5}

[a] Data from Ref. [61].

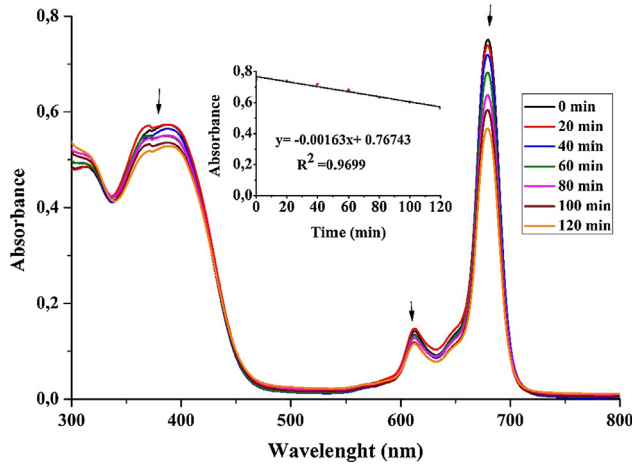

Fig. 6. Change observed in UV–vis spectrum during photodegradation quantum yield measurement of compound **4a** in DMSO.

occur. In the case of attachment of electron-withdrawing substituent groups to the phthalocyanine compound, oxidation of the phthalocyanine ring becomes more difficult and the photodegradation reaction becomes slower. Compound **4a** was dissolved in DMSO, UV–vis spectra were obtained by exposing the specimen to light at a specific time interval of 3.26×10^{16} photon s^{-1} cm^{-2}, and the changes in the Q band were examined (Fig. 6).

As a result of the photodegradation measurements of **4a**, only a decrease in the B and Q bands was observed in the spectrum and no new peak formation was observed. The photodegradation and quantum yield of compound **4a** are given in Table 4. The calculated Φ_d value was in accordance with the values in the literature. In the literature, compounds with photodegradation values in the range of 10^{-3} to 10^{-6} are considered stable [57].

3. Conclusions

Two novel phthalocyanines [M = Zn (**4a**) and M = Co (**4b**)] were synthesized using their corresponding metal salts and 4-(4-(3-(2,4,5-trimethoxyphenyl)acryloyl)phenoxy)-phthalonitrile as chalcone ligand (**4**), which was prepared from the reaction of 4-nitrophthalonitrile with 4-hydroxyphenyl-3-(2,4,5-trimethoxyphenyl)-prop-2-en-1-one (**3**). The newly synthesized phthalocyanines were characterized UV–vis, FT-IR, ^{1}H NMR, ^{13}C NMR, and MALDI-TOF mass spectra and elemental analysis.

When we titrate the **4a** complex with increasing DNA concentration, the fluorescence intensity is increased, but for the **4b** complex with increasing DNA concentration, the fluorescence intensity is decreasing. Enzyme inhibition activity was exhibited by **4a** for both enzymes. Compound **4b** exhibited inhibition activity against xanthine oxidase even in very small percentages, but carbonic anhydrase was inhibited by just **4a**. Zn^{2+} ion in the complex might compete with Zn of the enzyme active site.

The photochemical study of compound **4a** increased singlet oxygen production. In the photochemical study, both singlet oxygen production and photodegradation of compound **4a** increased in parallel with the literature. According to these results, compound **4a** may potentially be used for photodynamic therapy.

Although there are many photochemical studies in the literature, there is no study on the use of Pc-Co metal, due to the lack of data on the photochemical properties of compound **4b**. Furthermore, we could not obtain any data as a result of the photochemical measurements on.

4. Experimental section

4.1. Chemistry

4-Hydroxyacetophenone, 2,4,5-trimethoxybenzaldehyde, 4-nitrophthalonitrile, KOH, K_2CO_3, 1,8-diazabicyclo[5.4.0]undec-7-ene (DBU), $Zn(OAc)_2{\cdot}2H_2O$, $Co(OAc)_2{\cdot}4H_2O$, 1,3-diphenylisobenzofuran (DPBF), 4-nitrophenyl acetate (Sigma), xanthine (Sigma), potassium phosphate buffer, calf thymus DNA (CT-DNA) (Sigma), and uric acid were obtained from commercial suppliers. The solvents, such as acetone, DMF, DCM, DMSO, and ethanol, were dried and purified. ^{1}H NMR and ^{13}C NMR spectra were recorded in $CDCl_3$ (d 7.26 and 77.0 for ^{1}H and ^{13}C NMR, respectively) using a VARIAN Infinity Plus 300 MHz NMR spectrometer. UV–vis spectra were measured on a Shimadzu UV 2600 model spectrophotometer and infrared spectra were recorded on an Ati Unicam Mattson 1000 Series FT-IR (ATR system) spectrometer. MALDI-TOF spectra were recorded using Bruker Daltonics flexAnalysis. Fluorescence spectra were measured in a quartz cuvette using a Hitachi U-2910 and Fluoro Max-4 (Horiba Jobin Yvon), respectively. Elemental analysis was carried out using a LECO 932 CHNS-O apparatus. A General Electric halogen lamp (500 W) was used as light source. A 550-nm glass cut-off filter (Schott) and a water filter were used to filter off infrared and ultraviolet radiation, respectively.

4.1.1. Synthesis of 4-hydroxyphenyl-3-(2,4,5-trimethoxyphenyl)prop-2-en-1-one (3)

Chalcone (**3**) was prepared according to a method reported in the literature [15,44]. FT-IR max/cm^{-1}: 3284 cm^{-1} (OH); 3070 cm^{-1} (Ar—H); 2839 cm^{-1} (aliphatic C—H); 1655 cm^{-1} (C=O); 1598, 1576 cm^{-1} (Ar—C=C). ^{1}H NMR (300 MHz, CD_3OH): δ ppm 8.10 (d, J = 15.8 Hz, 1H, CH), 8.00 (d, J = 8.5 Hz, 1H, Ar—H), 7.50 (d, J = 5.8 Hz, 1H CH), 7.12 (bs, 1H, Ar—H), 6.90 (d, J = 8.8 Hz, 1H Ar—H), 6.52 (s, 1H, Ar—H), 3.94 (s, 3H, O—CH_3), 3.90 (s, 3H, O—CH_3) and 3.89 (s, 3H, O—CH_3). ^{13}C NMR (300 MHz, CD_3OH): δ ppm 190.43, 161.77, 154.80, 152.54, 143.30, 139.72, 131.25, 130.51, 120.12, 115.69, 115.52, 111.52, 96.96, 56.72, 56.52 and 56.20. Elemental analysis for [$C_{18}H_{18}O_5$]: C, 68.70; H, 5.71. Found: C, 68.78; H, 5.77%.

4.1.2. Synthesis of 4-(4-(3-(2,4,5-trimethoxyphenyl)acryloyl)phenoxy) phthalonitrile (4)

4-Nitrophthalonitrile (0.82 g, 4.77 mmol) and 4-hydroxyphenyl-3-(2,4,5-trimethoxyphenyl)prop-2-en-1-one (**3**) (1.5 g, 4.77 mmol) were dissolved in 25 mL of DMF. K_2CO_3 was added to the mixture over 15 min intervals and the mixture was stirred at 50 °C for 24 h under N_2 atmosphere. The reaction was stopped and then precipitated in iced water. It was filtered, washed with plenty of water, and then dried. A light yellow solid product was obtained. Yield: 1.86 g (86%). MW: 440.46. Mp: 193 °C. FT-IR max/cm^{-1}: 3069 cm^{-1} (Ar—H); 2939 cm^{-1} (aliphatic C—H); 2229 cm^{-1} (C≡N); 1656 cm^{-1} (C=O); 1608, 1584, 1560 cm^{-1} (C=C); 1025 cm^{-1} (C—O—C). ^{1}H NMR (300 MHz, $CDCl_3$): δ ppm 8.15 (d, J = 5.2 Hz, 1H CH), 8.10 (t, J = 2.0 Hz, 1H, Ar—H), 7.78 (d, J = 8.7 Hz, 1H CH), 7.48 (s, 1H, Ar—H), 7.43 (s, 1H, Ar—H), 7.37 (d, J = 2.5 Hz, 1H, Ar—H), 7.33 (d, J = 2.5 Hz, 1H, Ar—H), 7.19 (d, J = 2.4 Hz, 1H, Ar—H), 7.19 (1H, s, Ar—H), 7.17 (1H, s, Ar—H), 7.12 (1H, s, Ar—H), 3.95 (3H, s, O—CH_3), 3.92 (3H, s, O—CH_3) and 3.90 (3H, s, O—CH_3). ^{13}C NMR (300 MHz, $CDCl_3$): δ ppm 189.57, 160.96, 157.16, 155.11, 153.03, 143.47, 141.16, 136.84, 135.80, 131.43, 122.51, 122.34, 120.32, 119.70, 118.10, 115.44, 115.36, 115.00, 111.70, 109.96, 96.87, 56.80, 56.57 and 56.34. Elemental analysis for [$C_{26}H_{20}N_2O_5$]: C, 70.82; H, 4.51; N, 6.25. Found: C, 70.90; H, 4.58; N, 6.36%.

4.1.3. Synthesis of zinc (II) phthalocyanine (4a)

Compound **4** (0.2 g, 0.45 mmol) and $Zn(OAc)_2{\cdot}2H_2O$ (0.048 g, 0.22 mmol) were dissolved in 15 mL of DMF. Next, 2–3 drops of 1,8-diazabicyclo [5.4.0]-undec-7-ene (DBU) were added to the solution.

The reaction was then stirred for 24 h at 140 °C in a N_2 atmosphere. The mixture was precipitated in 100 mL of ice water. The precipitate was filtered, washed with hot water and hot alcohol, and dried. 0.10 g of dark green solid product was obtained. Yield: 48%. Mp > 350 °C. FT-IR ν_{max} (cm^{-1}): 3059 cm^{-1} (Ar—H); 2938 cm^{-1} (aliphatic C—H); 1650 cm^{-1} (C═O); 1595, 1567, 1504 cm^{-1} (C═N, C═C); 1027 cm^{-1} (C—O—C). UV–vis (DMF), λ_{max}, nm: 679, 615, 361. MALDI-TOF MS: *m/z* $[M]^+$ calc. for $C_{104}H_{80}N_8O_{20}Zn$: 1827.20; found $[M+H]^+$ 1828.10. Elemental analysis: C, 68.23; H, 4.33; N, 6.01. Found: C, 68.36; H, 4.41; N, 6.13%.

4.1.4. Synthesis of cobalt (II) phthalocyanine (4b)

Compound **4** (0.2 g, 0.45 mmol) and $Co(OAc)_2{\cdot}4H_2O$ (0.056 g, 0.22 mmol) were dissolved in 15 mL of DMF. Next, 2–3 drops of 1,8-diazabicyclo [5.4.0]-undec-7-ene (DBU) were added to the solution. The reaction was then stirred for 24 h at 140 °C in a N_2 atmosphere. The mixture was precipitated in 100 mL of ice water. The precipitate was filtered, washed with hot water and hot alcohol, and dried. 0.13 g of dark green solid product was obtained. Yield: 63%. Mp > 350 °C. FT-IR ν_{max}(cm^{-1}): 3069 cm^{-1} (Ar—H); 2943 cm^{-1} (aliphatic C—H); 1652 cm^{-1} (C═O); 1594, 1566, 1503 cm^{-1} (C═N, C═C); 1028 cm^{-1} (C—O—C). UV–vis (DMF), λ_{max}, nm: 676, 617, 387. MALDI-TOF MS: *m/z* $[M]^+$ calc. for $C_{104}H_{80}N_8O_{20}Co$: 1820.05; found $[M+H]^+$ 1821.20. Elemental analysis: C, 68.46; H, 4.33; N, 6.07. Found: C, 68.61; H, 4.43; N, 6.15%.

4.2. DNA-binding studies

4.2.1. Fluorescence spectroscopic studies

DNA-binding properties of complexes were investigated by fluorescence spectroscopic method. CT-DNA was used and a constant amount of complexes was titrated with an increasing amount of CT-DNA. The concentration of compounds was 10 μM and the CT-DNA concentration range was 15–100 μM for **4a** and 10.3–72 μM for **4b**. The reaction mixture was composed of CT-DNA and compounds in 5 mM Tris-HCl buffer (pH 7.4) and this mixture was incubated at 37 °C for 10 min. Excitation of compounds **4a** and **4b** was 348 and 361.6 nm, respectively. The emission wavelength of **4a** and **4b** was 684 nm. Fluorescence intensity of compounds binding to DNA was monitored at 684 nm. The DNA binding constant of compounds was calculated according to Eq. (1) [45]:

$$\log\frac{F_0-F}{F} = n\log K_a - n\log\frac{1}{[Q_t]-\frac{(F_0-F)[P_t]}{F_0}}, \quad (1)$$

where K_a and n are the binding constant and the number of binding sites in base pairs unit, respectively. F_0 and F are fluorescence intensity in the absence and presence of CT-DNA, and $[Q_t]$ and $[P_t]$ are the molar concentrations of DNA.

4.3. Enzyme inhibition assay

4.3.1. Xanthine oxidase assay

Xanthine oxidase activity in the presence of phthalocyanine complexes with metals such as Zn and Co was assayed by following uric acid formation. Xanthine was used as substrate. For the control reaction, reaction mixture (1 mL) containing 50 mM potassium phosphate buffer (pH 7.5), 0.051 mM xanthine, and 0.024 U xanthine oxidase was used. On the other hand, in the inhibitor reaction the mixture contained 0.125–40 μM phthalocyanine derivatives. The reaction mixtures were incubated at room temperature for 5 min and uric acid formation was monitored by measuring the absorbance at 290 nm. A buffer and xanthine mixture was used as blank. The inhibition percentage of xanthine oxidase activity was calculated according to Eq. (2):

$$\%\text{Xanthineoxidaseactivity} = \frac{(A_{control}-A_{sample})}{A_{control}} \times 100 \quad (2)$$

4.3.2. Carbonic anhydrase inhibition assay

Carbonic anhydrase was purified from human erythrocytes [47]. 4-Nitrophenyl acetate was used as substrate. The reaction mixture contained complexes between 1 and 10 μM for **4a** and 1 and 50 μM for **4b**, and 1 mM 4-nitrophenyl acetate from 3 mM stock and 20 mM Tris Sulfate (pH 7.4) from 50 mM Tris Sulfate (pH 7.4) and 0.32 U carbonic anhydrase isoform I. The enzyme activity was assayed by monitoring absorbance change at 348 nm for 3 min during 4-nitrophenolate forming as product. The control reaction mixture was the same except for complexes [48].

4.4. Singlet oxygen measurements

Compound **4a** was dissolved in DMSO. Then 1,3-diphenylisobenzofuran (concentration of DPBF: 3×10^{-5} mol/dm^3) was added as a singlet oxygen quencher. The UV–vis spectrum was obtained by exposing DPBF to a light intensity of 8.15×10^{15} photon s^{-1} cm^{-2} [58]. Eq. (3) was employed for the calculations:

$$\Phi_\Delta = \Phi_\Delta^{Std}\frac{R\cdot I_{abs}^{Std}}{R^{Std}\cdot I_{abs}}, \quad (3)$$

where Φ_Δ^{Std} is the singlet oxygen quantum yield (Φ_Δ) for the standard Zn-Pc (Φ_Δ^{Std} = 0.67 in DMSO) [59]. R and R^{Std} are the DPBF photobleaching rates in the existence of the respective samples (**4a**) and standard. I_{abs} and I_{abs}^{Std} are the rates of light absorption by the samples (**4a**) and standard.

4.4.1. Photodegradation and quantum yield

Photodegradation quantum yield (Φ_d) can be calculated by examining the change in fluorescence during the degradation of the light-interacting material. Photodegradation in phthalocyanines is determined by the decrease in the Q band and is calculated using the trends of the calibration graphs occurring at specific time intervals. Photodegradation quantum yield is calculated by the following Eq. (4) [60,61]:

$$\Phi_d = \frac{(C_0-C_t)\cdot V\cdot N_A}{I_{abs}\cdot S\cdot t}, \quad (4)$$

where C_0 is concentration of the sample before light application, C_t is concentration of the sample after light application, V is the volume used, N_A is the Avogadro constant, t is the irradiation time, S is the field of spectrophotometric cuvette used for irradiation, and I_{abs} is the power of the light used. A light intensity of 3.26×10^{16} photon s^{-1} cm^{-2} was employed for Φ_d determinations.

Conflict of interest

The authors confirm that this article content has no conflict of interest.

Acknowledgments

Many thanks for financial support of The Scientific and Technological Research Council of Turkey (TUBITAK, TBAG-113Z699 and KBAG-115Z446) and Sakarya University Scientific Research Projects Unit (SAU-BAP, Big Issue 2014-02-03-003). This study was carried out at Sakarya University Organic Chemistry Laboratory.

Appendix A. Supplementary material

Supplementary data associated with this article can be found, in the online version, at https://doi.org/10.1016/j.bioorg.2018.08.002.

References

[1] A. Mert Sevim, C. Ilgün, A. Gül, Preparation of heterogeneous phthalocyanine catalysts by cotton fabric dyeing, Dyes Pigments 89 (2011) 162–168.
[2] A. Yazıcı, N. Dalbul, A. Altındal, B. Salih, Ö. Bekaroğlu, Ethanol sensing property of novel phthalocyanines substituted with 3,4-dihydroxy-3-cyclobuten-1,2-dione, Sens. Actuat. B 202 (2014) 14–22.
[3] B.Y. Zheng, H.P. Zhang, M.R. Ke, J.D. Huang, Synthesis and antifungal photodynamic activities of a series of novel zinc (II) phthalocyanines substituted with piperazinyl moieties, Dyes Pigments 99 (2013) 185–191.
[4] T.V. Basova, A. Hassan, P.O. Krasnov, I. Gürol, V. Ahsen, Trimethylamine sorption into thin layers of fluoroalkyloxy and alkyloxy substituted phthalocyanines: optical detection and DFT calculations, Sens. Actuat. B 216 (2015) 204–211.
[5] M. Soylu, R. Ocaya, H. Tuncer, A.A. Al-Ghamdi, A. Dere, D.C. Sari, F. Yakuphanoglu, Analysis of photovoltaic behavior of Si-based junctions containing novel graphene oxide/nickel (II) phthalocyanine composite films, Microelectron. Eng. 154 (2016) 53–61.
[6] C.G. Chao, D.E. Bergbreiter, Highly organic phase soluble polyisobutylene-bound cobalt phthalocyanines as recyclable catalysts for nitroarene reduction, Catal. Commun. 77 (2016) 89–93.
[7] P. Sena, F. Dumludag, B. Salih, A.R. Özkaya, Ö. Bekaroglu, Synthesis and electrochemical, electrochromic and electrical properties of novel s-triazine bridged trinuclear Zn (II), Cu (II) and Lu (III) and a tris double-decker Lu (III) phthalocyanines, Synth. Met. 161 (2011) 1245–1254.
[8] M. Grobosch, C. Schmidt, R. Kraus, M. Knupfer, Electronic properties of transition metallophthalocyanines: the impact of the central metal atom (d^5–d^{10}), Org. Electron. 11 (2010) 1483–1488.
[9] H.A. Dinçer, A. Koca, A. Gül, M.B. Koçak, Novel phthalocyanines bearing both quaternizable and bulky substituents, Dyes Pigments 76 (2008) 825–831.
[10] C. Kantar, V. Mavi, N. Baltas, F. Islamoğlu, S. Şaşmaz, Novel zinc (II) phthalocyanines bearing azo-containing schiff base: determination of pKa values, absorption, emission, enzyme inhibition and photochemical properties, J. Mol. Struct. 1122 (2016) 88–99.
[11] G.K. Kantar, N. Baltaş, E. Menteşe, S. Şaşmaz, Microwave-assisted synthesis and investigation of xanthine oxidase inhibition of new phthalonitrile and phthalocyanines containing morpholino substituted 1,2,4-triazole-3-one, J. Organomet. Chem. 787 (2015) 8–13.
[12] Ü. Demirbaş, C. Göl, B. Barut, R. Bayrak, M. Durmuş, H. Kantekin, İ. Değirmencioğlu, Peripherally and non-peripherally tetra-benzothiazole substituted metal-free zinc (II) and lead (II) phthalocyanines: synthesis, characterization, and investigation of photophysical and photochemical properties, J. Mol. Struct. 1130 (2017) 677–687.
[13] V. Mantareva, M. Durmus, M. Aliosmana, I. Stoinevaa, I. Angelova, Lutetium (III) acetate phthalocyanines for photodynamic therapy applications: synthesis and photophysicochemical properties, Photodiagn. Photodyn. Ther. 14 (2016) 98–103.
[14] A. Modzelewska, C. Pettit, G. Achanta, N.E. Davidson, P. Huangb, S.R. Khana, Anticancer activities of novel chalcone and bis-chalcone derivatives, Bioorg. Med. Chem. 14 (2006) 3491–3495.
[15] B.S. Funiss, A.J. Hannford, P.W.G. Smith, A.R. Tatchell, Vogel's Textbook of Practical Org. Chem. fifth ed., Longman, London, 2004, pp. 1032–1035.
[16] H. Jin, X. Li, T. Tan, S. Wang, Y. Xiao, J. Tian, Electrochromic properties of novel chalcones containing triphenylamine moiety, Dyes Pigments 106 (2014) 154–160.
[17] P.S. Patil, S.R. Maidur, S.V. Rao, S.M. Dharmaprakash, Crystalline perfection, third-order nonlinear optical properties and optical limiting studies of 3,4-dimethoxy-4′-methoxychalcone single crystal, Opt. Laser Technol. 81 (2016) 70–76.
[18] K. Koran, F. Ozen, F. Biryan, K. Demirelli, A.O. Gorgulu, Eu^{+3}-doped chalcone substituted cyclotriphosphazenes: synthesis, characterizations, thermal and dielectrical properties, Inorg. Chim. Acta 450 (2016) 162–169.
[19] K. Koran, F. Ozen, G. Torğut, G. Pıhtılı, E. Cil, A.O. Gorgulu, M. Arslan, Synthesis, characterization and dielectric properties of phosphazenes containing chalcones, Polyhedron 79 (2014) 213–220.
[20] R. Gupta, R.P. Chaudhary, Synthesis, antimicrobial and DFT studies of novel fused thiazolopyrimidine derivatives, Heterocycl. Commun. 19 (2013) 207–214.
[21] A.L. Cole, S. Hossain, A.M. Cole, O. Phanstiel, Synthesis and bioevaluation of substituted chalcones, coumaranones and other flavonoids as anti-HIV agents, Bioorg. Med. Chem. 24 (2016) 2768–2776.
[22] G. Hu, X. Li, X. Zhang, Y. Li, L. Ma, L.M. Yang, G. Liu, W. Li, J. Huang, X. Shen, L. Hu, Y.T. Zheng, Y. Tang, Discovery of inhibitors to block interactions of HIV–1 integrase with human LEDGF/p75 via structure-based virtual screening and bioassays, J. Med. Chem. 55 (2012) 10108–10117.
[23] M. Rudrapal, R.S. Satyanandam, T.S. Swaroopini, T.N. Lakshmi, S.K. Jaha, S. Zaheera, Synthesis and antibacterial activity of some new hydrazones, Med. Chem. Res. 22 (2013) 2840–2846.
[24] C.T. Lın, K.J.S. Kumar, Y.H. Tseng, Z.J. Wang, M.Y. Pan, J.H. Xıao, S.C. Chıen, S.Y. Wang, Anti-inflammatory activity of flavokawain b from *Alpinia pricei* hayata, J. Agric. Food. Chem. 57 (2009) 6060–6065.
[25] Y.Y. Li, S.S. Huang, M.M. Lee, J.S. Deng, G.J. Huang, Anti-inflammatory activities of cardamonin from *Alpinia katsumadai* through heme oxygenase-1 induction and inhibition of NF-κB and MAPK signaling pathway in the carrageenan-induced paw edema, Int. Immunopharmacol. 25 (2015) 332–339.
[26] A.O. Gorgulu, K. Koran, F. Ozen, S. Tekin, S. Sandal, Synthesis, structural characterization and anti-carcinogenic activityof new cyclotriphosphazenes containing dioxybiphenyl and chalcone groups, J. Mol. Struct. 1087 (2015) 1–10.
[27] Y. Lee, B.S. Kim, S. Ahn, D. Koh, Y.H. Lee, S.Y. Shin, Y. Lim, Anticancer and structure-activity relationship evaluation of 3-(naphthalen-2-yl)-N,5-diphenyl-pyrazoline-1-carbothioamide analogs of chalcone, Bioorg. Chem. 68 (2016) 166–176.
[28] A. Kamal, N. Shankaraiah, S. Prabhakar, C.R. Reddy, N. Markandeya, K.L. Reddy, V. Devaiah, Solid-phase synthesis of new pyrrolobenzodiazepine–chalcone conjugates: DNA-binding affinity and anticancer activity, Bioorg. Med. Chem. Lett. 18 (2008) 2434–2439.
[29] H. Li, Y. Chen, B. Zhang, X. Niu, M. Song, Z. Luo, G. Lu, B. Liu, X. Zhao, J. Wang, X. Deng, Inhibition of sortase A by chalcone prevents *Listeria monocytogenes* infection, Biochem. Pharmacol. 106 (2016) 19–29.
[30] H. Wang, Y. Wang, Z. Chen, F.L. Chan, L.K. Leung, Hydroxychalcones exhibit differential effects on XRE transactivation, Toxicology 207 (2005) 303–313.
[31] B. Das, E. Tokunaga, M. Tanaka, T. Sasaki, N. Shibata, Perfluoroisopropyl zinc phthalocyanines conjugated with deoxyribonucleosides: synthesis, photophysical properties and in vitro photodynamic activities, Eur. J. Org. Chem. 15 (2010) 2878–2884.
[32] T. Keleş, B. Barut, Z. Biyiklioglu, A. Özel, A comparative study on DNA/BSA binding, DNA photocleavage and antioxidant activities of water soluble peripherally and non-peripherally tetra-3-pyridin-3-ylpropoxy-substituted Mn (III), Cu (II) phthalocyanines, Dyes Pigments 139 (2017) 575–586.
[33] M. Asadi, E. Safaei, B. Ranjbar, L. Hasani, Thermodynamic and spectroscopic study on the binding of cationic Zn (II) and Co (II) tetrapyridinoporphyrazines to calf thymus DNA: the role of the central metal in binding parameters, New J. Chem. 28 (2004) 1227–1234.
[34] W. Duan, Z. Wang, M.J. Cook, Synthesis of tetra(trimethylammonio)phthalocyanato zinc tetraiodide, $[ZnPc(NMe_3)_4]I_4$, and a spectrometric investigation of its interaction with calf thymus DNA, J. Porphyr. Phthalocya. 13 (2009) 1255–1261.
[35] C. Uslan, B.S. Sesalan, Synthesis of novel DNA-interacting phthalocyanines, Dyes Pigments 94 (2012) 127–135.
[36] H. Karaca, B. Çayetil, S. Sezer, Synthesis characterization and metal sensing applications of novel chalcone substituted phthalocyanines, Synth. Met. 215 (2016) 134–141.
[37] F. Aribi, C. Vey, D. Topkaya, S.T. Kostakoglu, J. Fournier-Dit-Chabert, S.I. Büyükeksi, G.C. Taskln, S. Alpugan, F. Albrieux, A.G. Gürek, M. Cucca, K. Bennis, D. Atilla, V. Ahsen, S. Ducki, F. Dumoulin, Phthalocyanine-chalcone conjugates, J. Porphyr. Phthalocya. 20 (2016) 497–504.
[38] A.A. Kaya, Synthesis, characterization and thermal behaviour of novel phthalocyanines bearing chalcone groups on peripheral positions, Bulg. Chem. Commun. 47 (2015) 844–848.
[39] D. Çakir, T. Arslan, Z. Biyiklioglu, An effect of the substituent position and metal type on the electropolymerization properties of chalcone substituted metallophthalocyanines, J. Chem. Soc. Dalton Trans. 44 (2015) 20859–20866.
[40] S. Tuncel, A. Trivella, D. Atilla, K. Bennis, H. Savoie, F. Albrieux, L. Delort, H. Billard, V. Dubois, V. Ahsen, F. Caldefie-Chézet, C. Richard, R.W. Boyle, S. Ducki, F. Dumoulin, Assessing the dual activity of a chalcone-phthalocyanine conjugate: design, synthesis, and antivascular and photodynamic properties, Mol. Pharm. 10 (2013) 3706–3716.
[41] A. Nas, N. Kahriman, H. Kantekin, N. Yayli, M. Durmuş, The synthesis of novel unmetallated and metallated phthalocyanines including (E)-4-(3-cinnamoylphenoxy) groups at the peripheral positions and photophysicochemical properties of their zinc phthalocyanine derivatives, Dyes Pigments 99 (2013) 90–98.
[42] J.T.F. Lau, X.-J. Jiang, D.K.P. Ng, P.-C. Lo, A disulfide-linked conjugate of ferrocenyl chalcone and silicon(iv) phthalocyanine as an activatable photosensitiser, Chem. Commun. 49 (2013) 4274–4276.
[43] S. Tuncel, J. Fournier-Dit-Chabert, F. Albrieux, V. Ahsen, S. Ducki, F. Dumoulin, Towards dual photodynamic and antiangiogenic agents: design and synthesis of a phthalocyanine-chalcone conjugate, Org. Biomol. Chem. 10 (2012) 1154–1157.
[44] S. Shenvi, K. Kumar, K.S. Hatti, K. Rijesh, L. Diwakar, G.C. Reddy, Synthesis, anticancer and antioxidant activities of 2,4,5-trimethoxy chalcones and analogues from asaronaldehyde: structureeactivity relationship, Eur. J. Med. Chem. 62 (2013) 435–442.
[45] M. Shakir, M. Azam, S. Parveen, A.U. Khan, F. Firdaus, Synthesis and spectroscopic studies on complexes of N,N′-bis-(2-pyridinecarboxaldimine)-1,8-diaminonaphthalene (L); DNA binding studies on Cu (II) complex, Spectrochim. Acta Part A 71 (2009) 1851–1856.
[46] W.Y. Li, J.G. Xu, X.Q. Guo, Q.Z. Zhu, Y.B. Zhao, Study on the interaction between rivanol and DNA and its application to DNA assay, Spectrochim. Acta Part A 53 (1997) 781–787.
[47] D. Ekinci, Ş. Beydemir, Z. Alım, Some drugs inhibit in vitro hydratase and esterase activities of human carbonic anhydrase-I and II, Pharmacol. R 59 (2007) 580–587.
[48] J.A. Verpoorte, S. Mehta, J.T. Edsall, Esterase activities of human carbonic anhydrases B and C, J. Biol. Chem. 242 (1967) 4221–4229.
[49] M.A. Rogawski, R.J. Porter, Antiepileptic drugs: pharmacological mechanisms and clinical efficacy with consideration of promising developmental stage compounds, Pharmacol. Rev. 42 (1990) 223–286.
[50] J.P. Richalet, M. Rivera, P. Bouchet, E. Chirinos, I. Onnen, O. Petitjean, A. Bienvenu, F. Lasne, S. Moutereau, F. Leon-Velarde, Acetazolamide a treatment for chronic mountain sickness, Am. J. Respir. Crit. Care. Med. 172 (2005) 1427–1433.
[51] M. Bozdag, F. Carta, D. Vullo, A. Akdemir, S. Isik, C. Lanzi, A. Scozzafava, E. Masini, C.T. Supuran, Synthesis of a new series of dithiocarbamates with effective human carbonic anhydrase inhibitory activity and antiglaucoma action, Bioorg. Med. Chem. 23 (2015) 2368–2376.
[52] F. Pacchiano, F. Carta, P.C. McDonald, Y. Lou, D. Vullo, A. Scozzafava, S. Dedhar, C.T. Supuran, Ureido-substituted benzenesulfonamides potently inhibit carbonic anhydrase IX and show antimetastatic activity in a model of breast cancer metastasis, J. Med. Chem. 54 (2011) 1896–1902.

[53] L.G. Smyth, G.O. Hurley, A.O. Grady, J.M. Fitzpatrick, E. Kay, R.W.G. Watson, Carbonic anhydrase IX expression in prostate cancer, Prostate Cancer P. D. 13 (2010) 178–181.
[54] C.T. Supuran, F. Briganti, S. Tilli, W.R. Chegwidden, A. Scozzafava, Carbonic anhydrase inhibitors: sulfonamides as antitumor agents, Bioorg. Med. Chem. 9 (2001) 703–714.
[55] C. Enroth, B.T. Eger, K. Okamoto, T. Nishino, T. Nishino, E.F. Pai, Crystal structures of bovine milk xanthine dehydrogenase and xanthine oxidase: structure-based mechanism of conversion, Proc. Natl. Acad. Sci. USA 97 (2000) 10723–10728.
[56] L.Z. Li, G.X. Zhou, J. Li, W. Jiang, B.L. Liu, W. Zhou, Compounds containing trace element copper or zinc exhibit as potent hyperuricemia inhibitors via xanthine oxidase inactivation, J. Trace Elem. Med. Biol. 49 (2018) 72–78.
[57] Y. Zorlu, F. Dumoulin, M. Durmuş, V. Ahsen, Comparative studies of photophysical and photochemical properties of solketal substituted platinum (II) and zinc (II) phthalocyanine sets, Tetrahedron 66 (2010) 3248–3258.
[58] A. Erdogmus, M. Durmus, A.L. Ugur, O. Avciata, U. Avciata, T. Nyokong, Synthesis, photophysics, photochemistry and fluorescence quenching studies on highly soluble substituted oxo-titanium (IV) phthalocyanine complexes, Synth. Met. 160 (2010) 1868–1876.
[59] P. Zimcik, M. Miletin, Z. Musil, K. Kopecky, L. Kubza, D. Brault, Cationic azaphthalocyanines bearing aliphatic tertiary amino substituents-synthesis, singlet oxygen production and spectroscopic studies, J. Photochem. Photobiol. A 183 (2006) 59–69.
[60] R. Bayrak, H.T. Akçay, M. Pişkin, M. Durmuş, İ. Değirmencioğlu, Azinebridged binuclear metallophthalocyanines functioning photophysical and photochemical-responsive, Dyes Pigments 95 (2012) 330–337.
[61] T. Nyokong, Effects of substituents on the photochemical and photophysical properties of main group metallophthalocyanines, Coord. Chem. Rev. 251 (2007) 1707–1722.